Detection of Oral Dysplasia in Animals with Fluorine-18-FDG and Carbon-11-Tyrosine

Jan W. Braams, Max J.H. Witjes, Corina A.A.M. Nooren, Peter G.J. Nikkels, Willem Vaalburg, Albert Vermey and Jan L.N. Roodenburg

Department of Oral and Maxillofacial Surgery, Department of Pathology, National Research PET Center, and Department of Surgical Oncology, Groningen University Hospital, Groningen, The Netherlands

The uptake of ^{18}F-fluorodeoxyglucose (FDG) and L-[1-^{11}C]tyrosine (TYR) was investigated in male Wistar albino rats with chemically induced dysplasia and oral squamous cell carcinoma (SCC) to correlate the uptake values with the grade of dysplasia. **Methods:** The palates of 54 rats was painted three times per week with 4-nitroquinoline 1-oxide to create different stages of dysplasia and SCC. After 2, 4, 6, 8, 12, 16, 20, 26 and 30 wk, these rats were investigated with PET. Immediately thereafter, the rats were killed and histologically prepared. Standardized uptake values (SUVs) of the palate of the rats were calculated and correlated with the Epithelial Atypia Index (EAI) and the thickness of the epithelial layer. **Results:** The TYR SUV correlated with the EAI and the epithelial thickness, 0.5 and 0.74, respectively. No correlation could be found for FDG SUV, compared to EAI and the epithelial thickness. **Conclusion:** For dysplasia and SCC, TYR showed higher uptake values than did FDG. It appeared that, for the detection of oral dysplasia, the tissue hyperplasia was more important than malignant features of dysplastic mucosa.

Key Words: PET; fluorodeoxyglucose; tyrosine; dysplasia

J Nucl Med 1998; 39:1476–1480

PET is currently under investigation as a tool for the detection of cancer. PET can accurately monitor the metabolic route of certain radioactive labeled nutrients, receptor ligands, drugs and other radiolabeled compounds. In this technique, the increased demand of tumor cells for certain nutrients is exploited to detect tumor tissue and to monitor therapy. Areas of high nutrient demand are displayed as areas with a high radioactive signal. The most widely used tracer is ^{18}F-fluorodeoxyglucose (FDG), with which it is possible to monitor the increased glucose metabolism in cancer cells. Over the years, the application of FDG showed that this tracer is not optimal in all cases (*1*). A drawback of FDG for the detection of tumor tissue is the uptake in inflammatory tissues (*2–4*). Also, in regions with a high basal metabolism, FDG is not very suitable (*5–8*). Nevertheless, the sensitivity and specificity of FDG PET to detect tumor tissue is often higher than that of CT, MRI or SPECT.

Jabour et al. (*9*) studied the potential of FDG in the detection of primary tumors and metastases in the head and neck region. They concluded that nonenlarged lymph nodes, negative for metastatic disease according to MRI and CT, can be detected by FDG PET. Braams et al. (*10*) concluded that FDG PET detects lymph node metastases with a high sensitivity (91%) and a somewhat lower specificity (88%). However, a substantial number of false-positive lymph nodes are usually detected by FDG PET. The positive predictive value of FDG PET is somewhat less than 50%. Despite the impressive sensitivity, the results of the FDG studies show that there is need for more cancer-specific tracers. Other metabolic processes were exploited, such as the rates of protein, ribonucleic acid or deoxyribonucleic acid synthesis (*11,12*). To visualize the protein synthesis rate, L-[1-^{11}C]-tyrosine (TYR) was introduced (*13*). The results of TYR PET in human studies are very promising in terms of sensitivity (83%) and specificity (95%) for the detection of several types of cancer (*14*). The positive predictive value of TYR PET was approximately 63%. The high uptake of TYR in the salivary glands and bone marrow impaired the results because the high signal from these normal tissues interferes with the detection of tumors in the vicinity.

Lindholm et al. (*15*) compared the uptake of FDG with the uptake of the amino acid L-[$^{11}CH_3$]methionine (MET) in head and neck cancer. Their results showed that there were no significant differences in tumor imaging between MET and FDG and that both tracers were very useful in the diagnosis of head and neck cancer. Braams et al. (*14*) studied the uptake of TYR in cervical lymph nodes in head and neck cancer and found a better specificity and accuracy with TYR than with FDG.

To enable the earliest possible treatment of squamous cell carcinoma (SCC), it is important to know at which point of development PET can detect the disease. It is known that oral epithelial dysplasia can be a preliminary state of SCC. We addressed this question with FDG and TYR in an oral dysplasia animal model. Oral epithelial dysplasia and SCC can be induced on the mucosa of the hard palate of the rat by repeated application of the carcinogen 4-nitroquinoline 1-oxide (4NQO). This autologous tumor model has advantages over transplanted models because it closely mimics human dysplasia and SCC (*16,17*). Furthermore, the grade of dysplasia can be numerically expressed by the Epithelial Atypia Index (EAI), as developed by Smith and Pindborg (*18*).

The aim of this study was to compare the potential value of FDG PET and TYR PET in the detection of oral dysplasia and cancer in the 4NQO rat palatal model.

MATERIALS AND METHODS

Animal Model

Dysplasias and SCCs were induced by the application of the carcinogen 4NQO on the mucosa of the hard palate of male Wistar albino rats. The palates of 8-wk-old rats were painted three times per week with 4NQO (0.5% wt/vol) solved in propylene glycol during a brief anesthesia with (a mixture) O_2/halothane/ethrane. After application, the rats were deprived of water for 2 hr to minimize the dilution effect. The rats were housed under standard conditions and were given standard rat pellets and water ad libitum.

When 4NQO is applied three times per week, highly differentiated SCC will develop within ~26 wk. During the application period, the tumors will be preceded by dysplasia of the oral epithelium. In general, the whole palatal mucosa is dysplastic. Tumors arise locally, and when the application is continued,

Received Aug. 26, 1997; revision accepted Nov. 13, 1997.

For correspondence or reprints contact: Jan W. Braams, DDS, Department of Oral and Maxillofacial Surgery, Groningen University Hospital, P.O. Box 30.001, 9700 RB Groningen, The Netherlands.

multifocal tumors are seen. The grading of the dysplasia is characterized by the EAI and correlated well with the extent of the application period (*19*). This experimental dysplasia is comparable with the human dysplasia and can be graded according to the EAI (*18*). For this study, 54 rats were divided into nine groups of six rats. The application durations with 4NQO for these different groups were 2, 4, 6, 8, 12, 16, 20, 26 and 30 wk.

PET Imaging

The camera used was a Siemens ECAT 951/31 whole-body machine (Siemens CTI, Knoxville, TN). The device acquires 31 planes across an axial length of 10.8 cm (slice thickness 0.35 cm). The measured resolution of the system is 5 mm at FWHM transaxiallly in the center of the field of view.

No-carrier-added FDG was synthesized with a radiochemical purity greater than 98%, according to Hamacher et al. (*20*). The TYR was produced by a remote-controlled synthesis of a non-carrier-added method via a microwave-induced Bücherer-Strecker synthesis (radiochemical purity 99%).

A transmission scan of 15 min was performed. After the injection of FDG or TYR, a dynamic emission scan of 40 min was made.

Calculation of the PET data was performed after individual reorientation and addition of the images. Briefly, the last three sagittal frames were added. These added sagittal PET images were individually reoriented to coronal and frontal planes to obtain a better view of the palate. The frontal planes containing the palate of the rat were added on an individual basis. A standardized elliptical region of interest was drawn on the hot spot representing the area of highest accumulation of the palate. Tracer accumulation was measured using standardized uptake values (SUVs):

$$\text{SUV} = \frac{\text{radioactivity concentration in region of interest (mCi} \cdot \text{cm}^{-3})}{\text{injected dose (mCi)/body weight (g).}} \quad \text{Eq. 1}$$

Experimental Procedure

Five rats died during the anesthesia procedure. The PET experiments were repeated with five other rats with an equivalent 4NQO treatment period at a later time.

For every stage of dysplasia and SCC, three rats were investigated with FDG, and three were investigated with TYR. Before the PET experiment, the fasting rats were anesthetized with an intraperitoneal injection of sodium pentobarbital (Euthesate). Three rats at the same time were positioned and fixed with tape in the camera on a what-not. Immediately after the transmission scan, FDG (range 0.2–0.5 mCi) or TYR (range 0.3–0.5 mCi) was injected into a lateral tail vein. The dose and, therefore, the injected volume were determined by the efficacy of the production yield of the tracer. Data acquisition was started immediately after administration of the tracer.

After the PET data acquisition, the rats were killed by an intracardial injection of sodium pentobarbital. Subsequently, the hard palate and a part of the soft palate were dissected and photographed. The dissected specimens were fixated in 4% (wt/vol) formalin and decalcified in a solution containing 25% (wt/vol) formic acid and 0.34 *M* trisodium-citrate-dihydrate for ~4 wk. The degree of decalcification was checked by radiographic analysis. After demineralization, the specimens were routinely processed and paraffin embedded. Histologic sections of 7 μm were cut in a sagittal plane at five different areas of the palate, namely, in front of the first molar, through the first molar, through the second molar, through the third molar and behind the third molar. The sections were stained with hematoxylin and eosin and examined by light microscopy. For each rat, an independent observer unaware of the PET results, assessed the EAI.

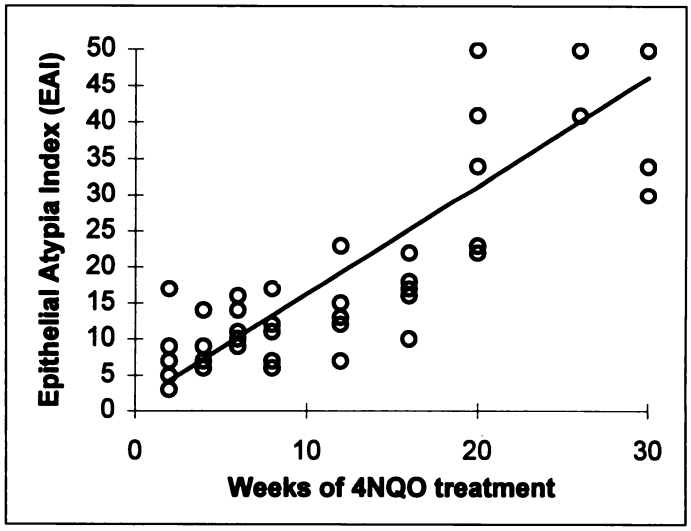

FIGURE 1. Results of histologic analysis of rat palatal mucosa treated with 4NQO using EAI. The correlation between the application period and the increase of dysplasia was 0.84 (n = 54).

Assessment of the Epithelial Thickness

During the analysis, it became apparent that the epithelial thickness possibly influenced the tracer accumulation (*21*). As a result of the 4NQO treatment, the thickness of the epithelial and keratin layer of the mucosa was increased. For that reason, the thickness of both layers was assessed on the same histologic slides used for EAI analysis by a morphometric system (Quantimed, Cambridge Systems, Cambridge, United Kingdom). For each rat, the average of three measurements was used.

RESULTS

Macroscopic Findings

During the whole experiment, the palates of the rats showed increasing changes of the mucosa. At up to 8 wk of 4NQO application, no gross macroscopic changes were observed in the palatal mucosa. From that time, a change of color of the palate to a more whitish aspect was detected. This whitening is probably the result of an increased keratinization and mild thickening of the mucosa. The topography of the palatal rugae was hardly disturbed. From that time on, the whitish thickening of the palatal mucosa increased, and a slight loss of definition appeared as short ridges and papillary growth all over the palatal mucosa. The rugal topography, however, was still discernible. As a result of the continuous application of 4NQO, the loss of normal structure gradually progressed. At week 26, exophytically growing epithelial lesions were observed. These lesions clinically presented as SCCs and were most pronounced in the gingival areas of the palate. These macroscopic results conform to the results of Nauta (*21*).

Microscopic Findings

The histologic changes of the palatal mucosa were graded with the EAI. The EAI of 4NQO-untreated rats was zero, indicating a total absence of epithelial dysplasia. In Figure 1, the EAI of the palatal mucosa is plotted against the weeks of 4NQO treatment. The EAI does not allow grading of SCC, and therefore, the number 50 was attributed to those palates with mucosa containing SCC. This is allowed because the Spearman test was used, which analyzes rank order. A good correlation relationship was present between the 4NQO application period and the EAI (Spearman analysis of rank order, correlation coefficient = 0.84, p = 0.0001). These results are in agreement with previous experiments with this tumor model (*21*).

FIGURE 2. A TYR PET image of two rats. A clear difference is visualized between the palate of the left rat (2-wk 4NQO treated) and the right rat (30-wk 4NQO treated).

During histologic analysis, it became apparent that the thickness of the epithelial layer was relevant to the amount of uptake. For that reason, we measured the epithelial thickness of the 4NQO-treated palatal mucosa. The correlation between the 4NQO treatment period and the increase of the epithelial thickness was 0.75 (Spearman analysis of rank order, $p < 0.0001$). In absolute measures, the thickness of the epithelial layer increased from 81 μm (normal untreated mucosa) to as much as 770 μm (mucosa treated for 30 wk with 4NQO).

PET Analyses

On the PET images, the palate was easy to locate because of its anatomical shape. There was no interference with the tracer uptake in the brain. The region of interest was any visually positive hot spot in the area of the palate. From the images, it appeared as if a clear difference between slight dysplastic mucosa and severe dysplasia or SCC could be observed (Fig. 2). However, a difference in uptake of FDG or TYR could not be confirmed by statistical analysis of the SUVs among the nine 4NQO treatment groups (Student–Newman–Keuls test).

With FDG, no relationship was found between the SUV of FDG and the EAI of the palatal mucosa (Fig. 3). The capricious pattern of SUVs of the rats injected with FDG was remarkable. In this group, the lowest mean SUV was found in the rats treated for 20 wk with 4NQO, whereas the highest mean SUV was found in rats treated for 12 wk.

There was no correlation found between the FDG SUV and the epithelial thickness (Fig. 4).

With the tracer TYR, statistical analysis showed that a correlation of 0.5 (Spearman analysis of rank order, $p < 0.0001$) existed between the TYR SUV and the EAI (Fig. 5).

Furthermore, a correlation of 0.74 was found between the TYR SUV and the increase of the epithelial thickness (Spearman analysis of rank order, $p < 0.0001$) (Fig. 6).

DISCUSSION

In this study, we examined the efficacy of FDG PET and TYR PET for the detection of dysplasia and oral SCC in an animal model. The induction of dysplasia and SCC in the palatal mucosa by 4NQO is accompanied by inflammatory reactions. In the first weeks, the inflamed tissues react with an increase of cellular response (*22*). There is often an increase of production of nasal fluids during the period of 4NQO induction. The presence of these tissue reactions may have influenced the FDG uptake. It has been well documented that FDG also accumulates in inflamed tissues (*2–4*). The histologic slides showed clear signs of inflammation in some rats with a high FDG SUV. This inflammation was mainly located at the basal

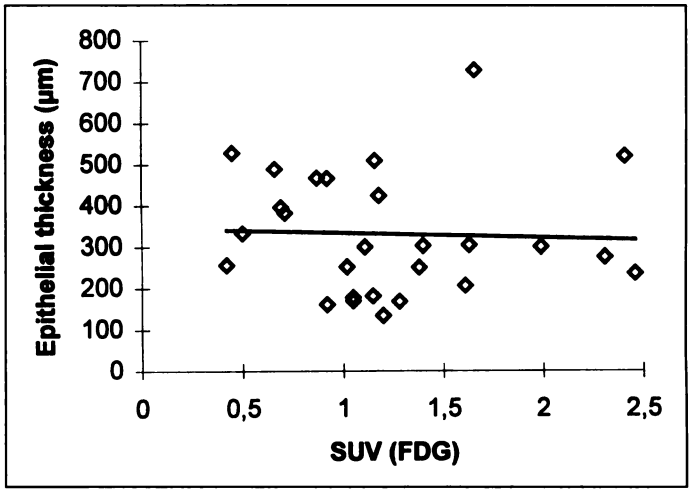

FIGURE 4. A plot of the SUVs of FDG versus the epithelial thickness (μm). No correlation could be calculated (n = 27). Line indicates trend of data.

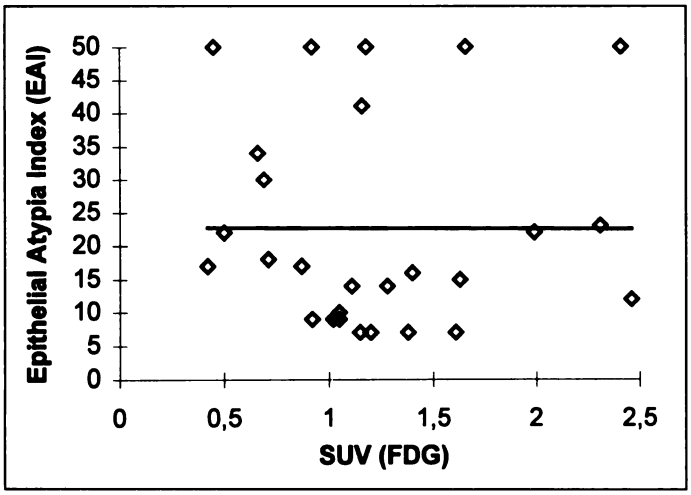

FIGURE 3. A plot of the SUVs of FDG versus the degree of dysplasia (EAI). No correlation could be calculated (n = 27). Line indicates trend of data.

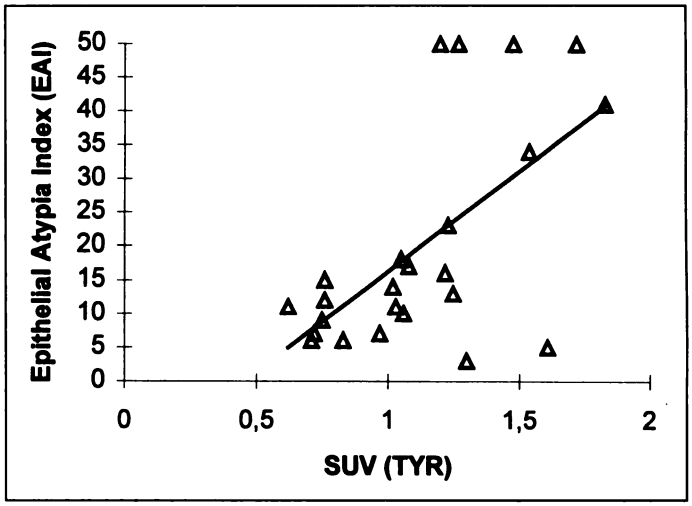

FIGURE 5. A plot of the SUVs of TYR versus the degree of dysplasia (EAI). A correlation of 0.5 was calculated (n = 27). Line indicates trend of data.

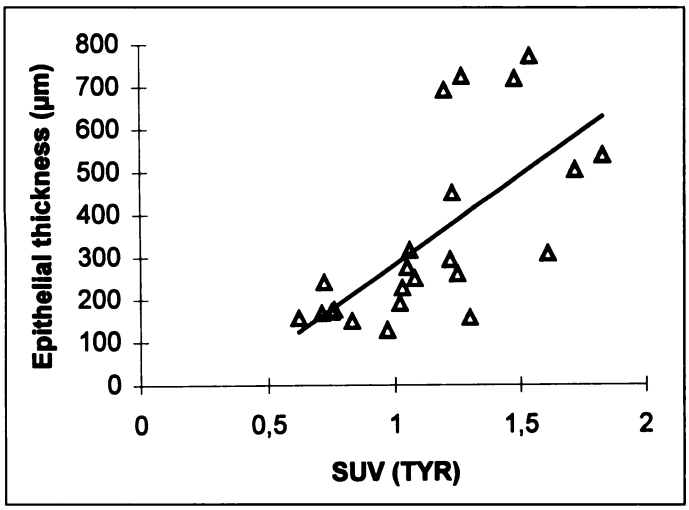

FIGURE 6. A plot of the SUVs of TYR versus the epithelial thickness (μm). A correlation of 0.74 was calculated (n = 27). Line indicates trend of data.

membrane of the epithelium (Fig. 7). These reactions also emphasize the capricious FDG uptake pattern. Because no correlation between the FDG SUV and the EAI was observed, it is concluded that FDG is not applicable as a tracer for the detection of dysplasia in the 4NQO rat palatal tumor model.

In contrast to FDG SUV, the TYR SUV showed a correlation with the EAI. The uptake of TYR was apparently less influenced by the presence of inflammatory tissue than the uptake of FDG. Because of the involvement of TYR in the protein synthesis, this was expected. Several investigations showed the selectivity of amino acids in cancer cells (*13*). However, two studies also showed the uptake of the amino acid MET in inflamed tissue (*23,24*).

A higher correlation was found between the thickness of the epithelial layer and the TYR SUV than between the EAI and the TYR SUV (0.74 versus 0.5). This remarkable difference was not anticipated. The increase of epithelial thickness due to the 4NQO treatment was comparable with the increase reported in other studies (*19*). As shown in Figure 5, the high uptake of TYR also occurred in hyperplastic tissue without severe dysplastic characteristics. Apparently, the increased protein demand in hyperplastic tissue was visualized by TYR PET. The histologic slides showed a large area of hyperplastic tissue (Fig. 8). It appeared that tissue hyperplasia is more important than the malignant features of dysplastic mucosa. No such correlation was found for FDG PET.

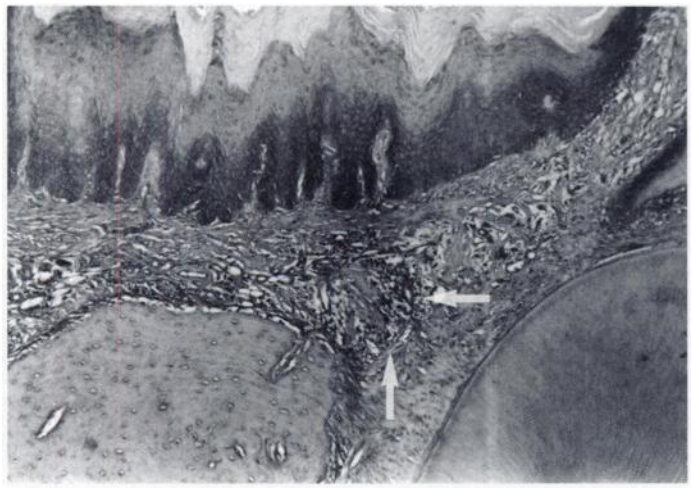

FIGURE 7. Photomicrograph of histologic section of a rat palate treated for 12 wk with 4NQO (×100). This rat showed a high uptake of FDG at the palate, despite the slight dysplastic changes. The histologic slide shows areas of clusters of inflammatory cells (arrows) and a diffuse spread of inflammatory cells in the stroma, probably responsible for the high FDG uptake.

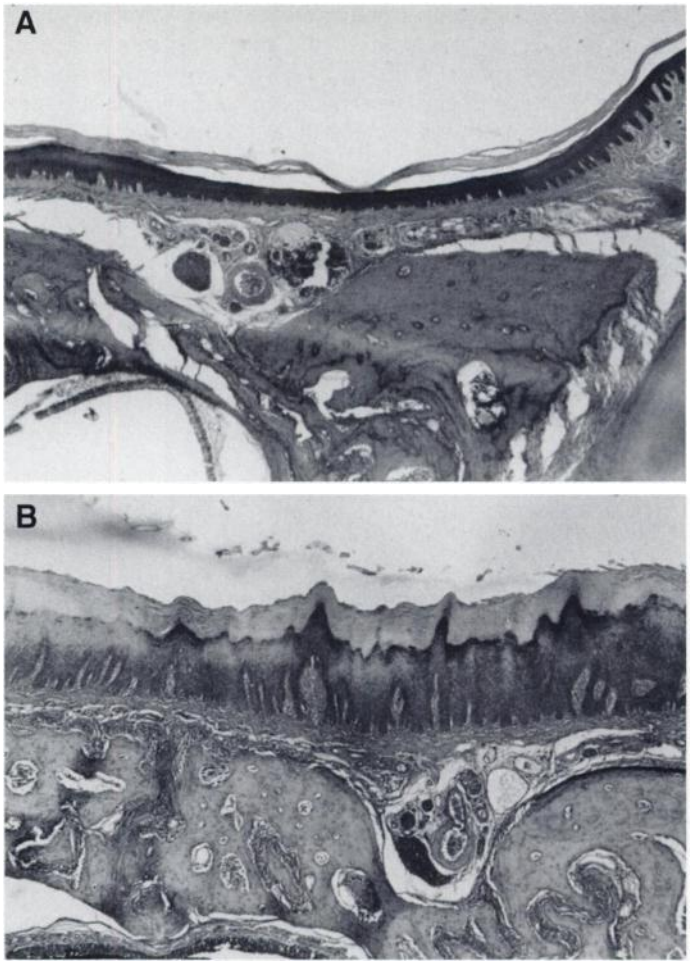

FIGURE 8. (A and B) Photomicrographs of histologic sections of a normal rat palate (A) and a rat palate treated for 2 wk with 4NQO (B) (both ×100). The 4NQO-treated rat showed a remarkably high uptake of TYR at the palate. The histologic slide showed an immoderate reactive hyperplasia, without inflammation, of the epithelium due to the 4NQO treatment. Normally, the dimensions of the epithelial layer in a rat treated for 2 wk with 4NQO are similar to the dimensions of normal epithelium.

Despite the small dimensions of the rat, the palate was easy to locate on the PET images. It can be argued that, because of the resolution of the PET camera, small malignant tumors cannot be visualized. In this study, we added three consecutive planes to obtain a clear picture of the palate of the rat. On average, the true dimensions of the palate are ~0.5 × 1 cm^2. The thickness of the epithelial layer varied from ~80 μm to 770 μm, depending on the 4NQO treatment period. This implies that the true volume of the investigated tissue was ~0.04–0.39 cm^3. The selectivity of TYR for hyperplastic tissue was relatively good, considering these small volumes. The results of FDG showed that this tracer cannot be applied in such small volumes. Due to the 4NQO-induced inflammation, the quantification of the FDG uptake was not reliable.

With PET, it is possible to detect severe dysplasia or early invasive carcinoma. It would be desirable that the uptake values beyond a certain threshold value would imply severe dysplasia or early carcinoma.

In this study, a cutoff point could be determined only for TYR. A SUV of 1.4 or higher would imply the presence of severe dysplasia or early invasive cancer (Fig. 5). Using this cutoff point, a sensitivity of 80% and a specificity of 89% could

be calculated. However, whether the results of these rat experiments can be extrapolated to the human situation remains unclear. All dysplasia induced by 4NQO will eventually turn into invasive carcinoma, whereas in humans, dysplasia (leucoplakia) does not always become invasive carcinoma (*21*).

CONCLUSION

Based on these experiments, it can be concluded that only the uptake of TYR and not of FDG correlated well with the grade of oral dysplasia and SCC. However, TYR uptake proved to correlate better with tissue hyperplasia than with the degree of malignancy. Also, in the 4NQO model, FDG PET suffered from high false-positive results due to the uptake in inflamed tissues. These results are in accordance with our clinical experience with FDG PET and TYR PET.

REFERENCES

1. Conti PS, Lilien DL, Hawley K, et al. PET and [^{18}F]-FDG in oncology: a clinical update. *Nucl Med Biol* 1996;6:717–735.
2. Sasaki M, Ichiya Y, Kuwabara Y. Ringlike uptake of [^{18}F]FDG in brain abscess: a PET study. *J Comput Assist Tomogr* 1990;14:486–487.
3. Kubota R, Yamada S, Kubota K, Ishiwata K, Tamahashi N, Ido T. Intratumoral distribution of fluorine-18-fluorodeoxyglucose in vivo: high accumulation in macrophages and granulation tissues studied by microautoradiography. *J Nucl Med* 1992; 33:1972–1980.
4. Wahl RL, Fisher SJ. A comparison of FDG, L-methionine and thymidine accumulation into experimental infections and reactive lymph nodes. *J Nucl Med* 1993;34:104P.
5. Ishiwata K, Takahashi T, Iwata R, et al. Tumor diagnosis by PET: potential of seven tracers examined in five experimental tumors including an artificial metastasis model. *Nucl Med Biol* 1992;19:611–618.
6. Hawkins RA, Phelps ME, Huang SC. Effects of temporal sampling, glucose metabolic rates and disruptions of the blood-brain barrier on the FDG model with and without a vascular compartment: studies in human brain tumors with PET. *J Cereb Blood Flow Metab* 1986;6:170–183.
7. Di Chiro G. Positron emission tomography using [^{18}F]fluorodeoxyglucose in brain tumors, a powerful diagnostic and prognostic tool. *Invest Radiol* 1987;22:360–371.
8. Ericson K, Lilja A, Bergstrom M, et al. Positron emission tomography with ([^{11}C]methyl)-L-methionine, [^{11}C]D-glucose, and [^{68}Ga]EDTA in supratentorial tumors. *J Comput Assist Tomogr* 1985;9:683–689.
9. Jabour BA, Choi Y, Hoh CK, et al. Extracranial head and neck: PET imaging with 2-[F-18]fluoro-2-deoxy-D-glucose and MR imaging correlation. *Radiology* 1993;186: 27–35.
10. Braams JW, Pruim J, Freling NJM, et al. Detection of lymph node metastases of squamous cell cancer of the head and neck with FDG PET and MRI. *J Nucl Med* 1995;36:211–216.
11. Vaalburg W, Coenen HH, Crouzel C, et al. Amino acids for the measurement of protein synthesis in vivo by PET. *Nucl Med Biol* 1992;19:227–237.
12. Phelps ME, Barrio JR, Huang SC, Keen RE, Chugani H, Mazziotta JC. Criteria for the tracer kinetic measurement of cerebral protein synthesis in humans with positron emission tomography. *Ann Neurol* 1984;15(suppl):S192–S202.
13. Willemsen ATM, van Waarde A, Paans AMJ, et al. In vivo protein synthesis rate determination in primary or recurrent brain tumors using L-[1-^{11}C]-tyrosine and PET. *J Nucl Med* 1995;36:411–419.
14. Braams JW, Pruim J, Nikkels PGJ, et al. Nodal spread of squamous cell carcinoma of the oral cavity detected with PET-tyrosine, MRI and CT. *J Nucl Med* 1996;37:897–901.
15. Lindholm P, Leskinen-Kallio S, Minn H, et al. Comparison of fluorine-18-fluorodeoxyglucose and carbon-11-methionine in head and neck cancer. *J Nucl Med* 1993;34: 1711–1716.
16. Nauta JM, Roodenburg JLN, Nikkels PGJ, Witjes MJH, Vermey A. Comparison of epithelial dysplasia: the 4NQO rat palatal model versus human oral mucosa. *Int J Oral Maxillofac Surg* 1995;24:53–58.
17. Prime SS, Malamos D, Rosser TJ, Scully CM. Oral epithelial atypia and acantholytic dyskeratosis in rats painted with 4-nitroquinoline N-oxide. *J Oral Pathol* 1986;15: 280–283.
18. Smith CJ, Pindborg JJ. *Histological grading of oral epithelial atypia by the use of photographic standards.* Copenhagen: Hamburger C; 1969.
19. Nauta JM, Roodenburg JLN, Nikkels PGJ, Witjes MJH, Vermey A. Epithelial dysplasia and squamous cell carcinoma of the Wistar rat palatal mucosa: the 4NQO model. *Head Neck* 1996;18:441–449.
20. Hamacher K, Coenen HH, Stöcklin G. Efficient stereospecific synthesis of no-carrier-added 2-[^{18}F]-fluoro-2-deoxy-D-glucose using aminopolyether supported nucleophilic substitution. *J Nucl Med* 1986;27:235–238.
21. Nauta JM. Photodynamic therapy and photodetection of dysplastic lesions and squamous cell carcinomas of the oral mucosa [PhD thesis]. Groningen; University of Groningen; 1996.
22. Fisker AV. Chemically induced experimental oral carcinogenesis: establishment of an experimental model based on application of the carcinogen 4-nitroquinoline n-oxide on the palatal mucosa of rats [PhD thesis]. Aarhus; Royal Dental College; 1978.
23. Leskinen-Kallio S, Någren K, Lehikoinen P, Ruotsalainen U, Joensuu H. Uptake of ^{11}C-methionine in breast cancer studied by PET: an association with the size of S-phase fraction. *Br J Cancer* 1991;64:1121–1124.
24. Kubota K, Matsukawa T, Fujiwara T, et al. Differential diagnosis of lung tumor with positron emission tomography: a prospective study. *J Nucl Med* 1990;31:1927–1933.